

Dynamic Numerical Simulation Model of Supercritical CO₂ Pipeline Containing Impurities

Jianxin Lu¹, Qihui Hu^{1*}, Qing Miao², Yuxing Li^{1*}, Chaofei Nie², Xin Ouyang², Jianlu Zhu¹, Qiyun Jia¹

1.China University of Petroleum (East China)

2. National Petroleum and Natural Gas Pipeline Network Group Science and Technology Research Institute Branch

(*Qihui Hu: huqihui_upc@126.com; * Yuxing Li: liyx@upc.edu.cn)

ABSTRACT

This study established a one-dimensional dynamic simulation model for a supercritical carbon dioxide pipeline containing impurities. By using C++ programming and numerical solution technology, the hydraulic and thermal properties of the pipeline during slow transient operating conditions can be calculated, enabling dynamic monitoring of the hydraulic and thermal properties along the pipeline during the transportation of impurities in supercritical carbon dioxide. The comparison and verification between the current authoritative engineering simulation software OLGA and this model indicate that the model has certain engineering application value and has reference significance for the development of domestic simulation software.

Keywords: CCUS, supercritical CO₂ pipeline, slow transient flow, numerical solution technology, C++ programming

NOMENCLATURE

| | |
|------|---|
| A | area(m ²) |
| D | pipe diameter (m) |
| f | friction factor |
| h | specific enthalpy (J/kg) |
| K | overall heat-transfer coefficient(W/(m ² K)) |
| Ke | pipe roughness (mm) |
| M | mass flow rate (kg/s) |
| n | number of pipeline discretization sections |
| P | gas pressure (Pa) |
| q | rate of heat transfer per unit time and unit mass |

| | |
|-------|----------------------------------|
| R | specific gas constant (J/(kg K)) |
| Re | Reynolds number |
| t | time (s) |
| T | gas temperature (K) |
| T_0 | temperature of the ground (K) |
| w | flow velocity (m/s) |
| x | spatial coordinate(m) |

Greek symbols

| | |
|-----------|---|
| λ | heat conductivity (W/(m K)) |
| ρ | density of the gas (kg/m ³) |

1. INTRODUCTION

Carbon Capture, Utilization and Storage (CCUS) is the most direct technical way to achieve carbon peaking and carbon neutrality, and pipeline transportation plays a vital role in the CCUS technology 错误!未找到引用源。 Supercritical carbon dioxide, which is a state where the fluid has both liquid-like and gas-like properties, is the primary medium used for carbon dioxide transportation due to its favorable properties, such as high density and low viscosity. Moreover, the compression coefficient of CO₂ in the supercritical state changes only slightly and tends to stabilize during transportation, which reduces energy consumption. Additionally, supercritical CO₂ has lower thermal conductivity and smaller fluctuation amplitudes than its gas or liquid phases, making it ideal for pipeline insulation during transportation^[1]. Therefore, the use of supercritical CO₂ for pipeline transportation has become the mainstream method for transporting

carbon dioxide in the CCUS industry.

The carbon dioxide long-distance pipeline in CCUS often experiences dynamic fluctuations in the hydraulic and thermal conditions inside the pipeline due to unstable gas source output or fluctuations in user usage, which belongs to slow transient conditions. At the same time, CO₂ during transportation often contains various impurities, which affect the properties of the medium and subsequently affect the changes in hydraulic and thermodynamic parameters during the transportation process.

Currently, there is extensive research on transient simulation of oil and gas pipeline transportation, but research on transient simulation of supercritical CO₂ pipeline transportation is relatively scarce. Commercial simulation software, such as Fluent, CFX, and OLGA, are commonly used for this purpose. For instance, Chen Bing's team^[3] from Xi'an Petroleum University used OLGA and Fluent software to study the characteristics of CO₂ pipeline transportation process. In terms of programming modeling research, Gu Shuaiwei^[7] used MATLAB programming to establish the calculation model of decompression wave propagation in the process of supercritical CO₂ pipeline leakage, in which the physical property calculation part is calculated by calling NIST-REFPROP dynamic link library. Maciej Chaczykowski^[8] established a dynamic simulation model for supercritical/dense phase CO₂ pipelines containing impurities. The model also calls for data from the NIST-REFPROP dynamic link library in terms of physical property calculation and related partial derivatives, and uses a DASSL solver for solution. Li Changjun's team^[9] established a simulation model for natural gas pipeline network systems suitable for any structural form based on the principles of mass conservation, momentum conservation, energy conservation, and non-pipe component characteristic equations. Given the high demands placed on the theoretical underpinnings, mathematical approaches, and programming skills required to construct a flow simulation model through programming alone, there exists a paucity of research on the application of numerical solution techniques to simulate the transportation of supercritical carbon dioxide through pipeline networks using autonomous programming modeling. Nevertheless, this avenue represents a critical approach to advancing the precision

and effectiveness of simulation calculations.

Although commercial simulation software is relatively mature in the field of transient flow calculation in oil and gas pipelines, simulating supercritical CO₂ pipelines is challenging due to their unique properties. Moreover, the development of domestically produced CFD simulation software in China is still in its early stages. Although some domestic simulation platforms have been applied in engineering and research, there is still a significant gap compared to foreign countries, particularly in terms of transient calculation for supercritical CO₂ pipelines. Autonomous programming, modeling, and computing are critical components of building simulation platforms and are necessary for achieving software localization.

The primary purpose of this study is to develop a one-dimensional transient compressible flow model that is suitable for supercritical CO₂ pipelines through autonomous programming modeling, and to enable real-time monitoring of hydraulic and thermal changes during slow transient operating conditions of pipelines. The model is based on the one-dimensional compressible viscous flow Euler equation as the control equation, and it combines the PR state equation and its enthalpy equation to form a complete theoretical model system. We applied this model to simulate the hydraulic and thermal dynamic changes along the supercritical CO₂ pipeline with impurities under dynamic change conditions. Furthermore, the accuracy of the model was verified through comparisons and analysis of the calculation results with those obtained using the OLGA software.

2. THEORETICAL MODEL

2.1 Basic equation

The basic equations are derived from the conservation principles. For one-dimensional, compressible fluid flow without considering terrain fluctuations and viscous forces we have

Continuity equation

$$\frac{\partial \rho}{\partial \tau} + \frac{\partial(\rho \omega)}{\partial x} = 0 \quad (1)$$

Equation of momentum

$$\frac{\partial(\rho\omega)}{\partial\tau} + \frac{\partial(P + \rho\omega^2)}{\partial x} + \frac{\rho\omega^2 f}{2D} = 0 \quad (2)$$

Energy equation

$$\begin{aligned} & \frac{\partial}{\partial t}[\rho(e + \frac{w^2}{2})] + \frac{\partial}{\partial x}[\rho(e + \frac{w^2}{2})w] \\ & = \rho q + \frac{\partial q_x}{\partial x} - \frac{\partial(wP)}{\partial x} \end{aligned} \quad (3)$$

where ρ is the density of the medium, w is the flow rate, P is the medium pressure, D is the inner diameter of the pipeline, f is the friction factor, q is the volumetric heating rate per unit mass, q_x is the heat flow rate in the flow direction, and e is the internal energy.

The friction coefficient is obtained from the Colebrook–White equation^[10]

$$\frac{1}{\sqrt{f}} = -2 \lg\left(\frac{Ke}{3.7D} + \frac{2.51}{Re\sqrt{f}}\right) \quad (4)$$

where Ke is pipe roughness, Re is Reynolds number. This formula is applicable to the calculation of turbulent flow area and is the most accurate formula for calculating hydraulic friction coefficient at present. In this paper, during transportation, the medium flow is close to the resistance square area. Thus, the influence of Reynolds number is ignored, and the above formula (4) is simplified as

$$\frac{1}{\sqrt{f}} = -2 \lg \frac{Ke}{3.7D} \quad (5)$$

The internal energy: $e = h - P/\rho$, after bringing it in (3) and simplifying we obtain

$$\begin{aligned} & \frac{\partial}{\partial t}[\rho(h - \frac{P}{\rho} + \frac{w^2}{2})] + \frac{\partial}{\partial x}[\rho(h + \frac{w^2}{2})w] \\ & = \rho q + \frac{\partial q_x}{\partial x} \end{aligned} \quad (6)$$

where h is the enthalpy of the medium. ρq is the volume heating (radiation heat, etc.), which is not considered in this article, $\frac{\partial q_x}{\partial x}$ represents the thermal transport across the surface caused by temperature gradients, which is the heat exchange with the surrounding environment through heat conduction. For pipelines, it can be expressed as^[11]

$$\frac{\partial q_x}{\partial x} = -\frac{4K(T - T_0)}{D} \quad (7)$$

where K is the overall heat-transfer coefficient, T is the medium temperature, and T_0 is the environment temperature.

The overall heat-transfer coefficient for large diameter buried pipelines without insulation layer is calculated from the expression^[11]:

$$K = \frac{2\lambda_t}{D_w \ln\left[\frac{2H}{D_w} + \sqrt{\left(\frac{2H}{D_w}\right)^2 - 1}\right]} \quad (8)$$

Where λ_t is the soil thermal conductivity, H is the

buried depth of the pipeline, and D_w is the outer diameter of the pipeline

After substituting (5) into (4), we obtain

$$\begin{aligned} & \frac{\partial}{\partial t}[\rho(h - \frac{P}{\rho} + \frac{w^2}{2})] + \frac{\partial}{\partial x}[\rho(h + \frac{w^2}{2})w] \\ & + \frac{4K(T - T_0)}{D} = 0 \end{aligned} \quad (9)$$

This is the final form of the energy equation in this article

2.2 Equation of state

To close the set of equations presented in Section 2.1, an equation of state must be employed. In this study, the Peng-Robinson (PR) equation of state was utilized to calculate the density and its derivatives with respect to pressure and temperature, employing its mixture model. This equation of state is a cubic equation and is frequently utilized in engineering calculations owing to its simplicity and accuracy.

The PR equation of state can be expressed as a cubic polynomial form of the specific volume V

$$\begin{aligned} & V^3 + \left(b - \frac{RT}{P}\right)V^2 + \frac{a - 2RTb - 3Pb^2}{P} \cdot V \\ & + \frac{RTb^2 - ab}{P} + b^3 = 0 \end{aligned} \quad (10)$$

The specific volume is obtained from the iterative solution of (10) using Newton's method. And then, the density is calculated from the expression:

$$\rho = \frac{1000M_{mix}}{V} \quad (11)$$

where M_{mix} is the molar mass of the CO₂ mixture.

The calculation of enthalpy is

$$h = h_0 + h_r \quad (12)$$

where h_0 is the enthalpy of ideal gas and h_r is the residual enthalpy.

The enthalpy of ideal gas is calculated from the expression^[12]:

$$h_0 = A + BT + CT^2 + DT^3 + ET^4 \quad (13)$$

The residual enthalpy calculation equation based on the PR equation is

$$h_r = \frac{(T\beta - a)}{2\sqrt{2}b} \ln \frac{v - 0.414b}{v + 2.414b} \quad (14)$$

$$+RT - pv$$

which is derived from reference [14]^[14]. The meaning and calculation of parameters in (14) refer to reference [13]^[13].

2.3 The model for steady state calculation

In theoretical terms, the initial conditions have a minimal impact on the numerical calculation results of transient problems. However, in practical numerical calculations, inappropriate initial conditions can negatively affect the convergence speed and even lead to computational divergence. Therefore, using the steady-state calculation results as the initial condition for transient simulation is beneficial for improving the speed

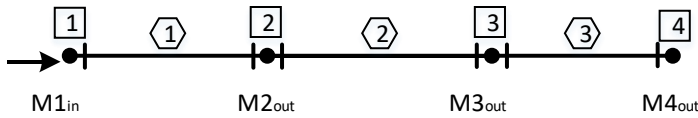


Fig. 1. Transmission process of simple pipeline.

and stability of transient calculation. It is necessary to calculate the hydraulic and thermal distribution of the pipeline during steady-state operation before transient calculation to ensure proper initial conditions for the transient simulation.

Based on the fundamental equation presented in Section 2.1, the equation for steady-state calculation can

be obtained by eliminating the time term in the fundamental equation. The equations for steady-state flow are all ordinary differential equations in terms of distance. By incorporating the PR equation of state and its enthalpy calculation equation, the continuity, momentum, and energy equations for one-dimensional steady-state flow in pipelines can be expressed as follows:

$$\begin{bmatrix} a_{11} & a_{12} & a_{13} \\ a_{21} & a_{22} & a_{23} \\ a_{31} & a_{32} & a_{33} \end{bmatrix} \begin{bmatrix} \frac{dT}{dx} \\ \frac{dP}{dx} \\ \frac{dw}{dx} \end{bmatrix} = \begin{bmatrix} b_1 \\ b_2 \\ b_3 \end{bmatrix} \quad (15)$$

$$\text{where: } a_{11} = \frac{w}{\rho} \left(\frac{\partial \rho}{\partial T} \right)_p, a_{12} = \frac{w}{\rho} \left(\frac{\partial \rho}{\partial P} \right)_T, a_{13} = 1, b_1 = 0; a_{21} = 0, a_{22} = \frac{1}{\rho}, a_{23} = w, b_2 = -\frac{w^2 \lambda}{2D}; a_{31} = \left(\frac{\partial h}{\partial T} \right)_p, a_{32} = \left(\frac{\partial h}{\partial P} \right)_T, a_{33} = w, b_3 = -\frac{4K(T-T_0)}{\rho w D}.$$

2.4 The model for slow transient state calculation

In this section, Eqs. (1), (2) and (9) are rewritten with density, temperature and mass flow rate as the dependent variables. Using the identity $w = M \rho^{-1} A^{-1}$ into Eqs. (1), (2) and (9), we obtain^[15]

$$\frac{\partial \rho}{\partial \tau} + \frac{1}{A} \frac{\partial M}{\partial x} = 0 \quad (16)$$

$$\frac{\partial M}{\partial \tau} + \frac{1}{A} \frac{\partial \left(A^2 P + \frac{M^2}{\rho} \right)}{\partial x} + \frac{\lambda M |M|}{2DA\rho} = 0 \quad (17)$$

$$\frac{\partial}{\partial t} \left[\rho \left(h - \frac{P}{\rho} + \frac{M^2}{2\rho^2 A^2} \right) \right] + \frac{1}{A} \frac{\partial}{\partial x} \left[\left(h + \frac{M^2}{2\rho^2 A^2} \right) M \right] + \frac{4K(T-T_0)}{D} = 0 \quad (18)$$

To ensure closure of the set of equations in this model, boundary conditions must be applied. Typically, the number of unknowns to be solved is greater than the

number of difference equations, necessitating the use of boundary conditions. For this study, it is assumed that the temperature and pressure at the pipeline inlet, as well as the flow rate at the outlet, are known. Additionally, the density-temperature values at intersection nodes of pipeline sections are considered equal and the sum of flow rates is zero. These assumptions serve as the necessary boundary conditions for solving the model equations.

The transmission process of simple pipeline shown in Fig. 1 has three segments and four nodes. Node 1 is the gas source point, and nodes 2 and 3 each have gas distribution volumes $M_{2,out}$, $M_{3,out}$ and $M_{4,out}$. To establish the hydraulic and thermodynamic calculation model for pipeline transportation, the pipeline system is divided into several segments, and each segment is further divided into several calculation sections. In this study, the transmission process of a simple pipeline, shown in Fig. 1, consists of three segments and four nodes, where node 1 is the starting point, nodes 2 and 3 are the intermediate gas distribution points, and node 4 is the end point. The intake volume is denoted as x , and the gas distribution volume of the node is denoted as y . Each calculation section has three variables, namely, density (ρ), temperature (T), and mass flow rate (M), resulting in a total of eighteen unknown variables across the six calculated cross-sections. The establishment of three difference equations per pipe section and nine difference equations for the entire pipeline system requires nine boundary conditions. In this model, the boundary conditions include the pressure and temperature at the starting point of the pipeline, the flow rate at the end point of the pipeline, and the temperature density at the intersection nodes of the pipeline section, where the sum of the flow rates is zero.

$$BF_1 = P_{1,1} - const = 0 \quad (19)$$

$$BF_2 = T_{1,1} - const = 0 \quad (20)$$

$$BF_3 = \rho_{1,2} - \rho_{2,1} = 0 \quad (21)$$

$$BF_4 = \rho_{2,2} - \rho_{3,1} = 0 \quad (22)$$

$$BF_5 = T_{1,2} - T_{2,1} = 0 \quad (23)$$

$$BF_6 = T_{2,2} - T_{3,1} = 0 \quad (24)$$

$$BF_7 = M_{2,out} + M_{2,1} - M_{1,2} = 0 \quad (25)$$

$$BF_8 = M_{3,out} + M_{3,1} - M_{2,2} = 0 \quad (26)$$

$$BF_9 = M_{4,out} - M_{3,2} = 0 \quad (27)$$

Specifically, Eqs. (19) and (20) represent the boundary conditions at the starting point of the pipeline, where it is assumed that the temperature and pressure remain constant. Eqs. (21) to (26) represent the boundary conditions at the nodes of the pipeline segment, where it is assumed that there are no temperature and pressure changes in the connected section, and the temperature and density before and after the node remain constant, with inflow equal to outflow. Finally, Eq. (27) represents the boundary condition at the end of the pipeline, where inflow is equal to outflow at the node. In total, nine boundary conditions need to be established to close the system of difference equations.

Based on the pipeline segmentation method, the number of unknown variables to be solved can be determined. If the pipeline is divided into n segments for calculation, the total number of unknown variables to be solved is $6n$. Each segment can establish three difference equations, resulting in a total of $3n$ difference equations. In this study, $3(n-1)$ boundary conditions are applied at the intersection nodes of each pipeline segment, while two boundary conditions are applied at the beginning of the pipeline, and one boundary condition is applied at the end of the pipeline. The total number of boundary conditions is $3n$, which makes the equation system closed.

3. SOLUTION METHOD

The numerical solution process for supercritical CO₂ pipelines can be divided into two parts. The first part involves solving the one-dimensional steady-state hydraulic and thermodynamic calculation using the explicit fourth-order Runge-Kutta method, which has high accuracy and numerical stability. This method produces the hydraulic and thermal distribution along the pipeline under steady-state operation. The second part involves solving the one-dimensional slow transient hydraulic and thermal calculation using the implicit

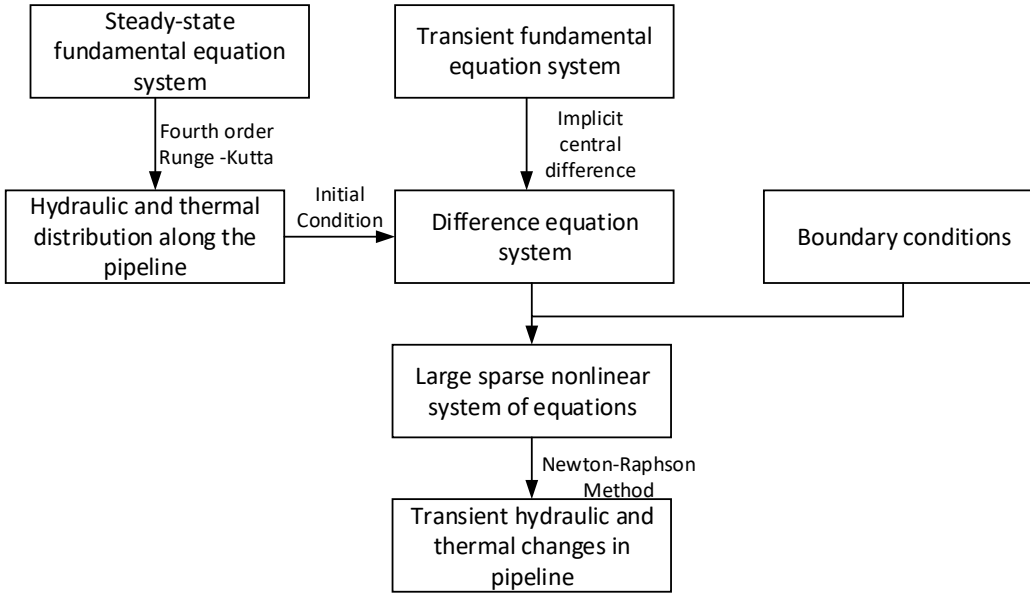


Fig. 2. Numerical calculation flow

central difference method. This method discretizes the continuity equation, motion equation, and energy equation under transient conditions, with the steady-state calculation results serving as the initial values. This method is suitable for slow transient flow simulation processes with large time steps, without strict requirements for time step size, while maintaining numerical stability. However, when dealing with fast transient problems, false spatial numerical oscillations may occur. The implicit central difference method is used to transform the original large-scale nonlinear partial differential equation into large-scale nonlinear algebraic equation. As the equations are non-linear and easy to derive the derivatives, and it is easy to give the initial value of the iteration, the Newton-Raphson iterative method is used to solve the equations. This method enables the dynamic monitoring of hydraulic and thermal changes within the pipeline during the specified time period. The calculation process of this study is illustrated in Fig. 2, and its details are explained in the following sections.

3.1 Numerical solution of steady-state flow

In this study, the explicit fourth order Runge-Kutta method is utilized to solve the steady-state hydraulic and thermodynamic calculation of supercritical CO₂ pipelines, which requires solving the (15) linear equation system.

The Gaussian Seidel iteration method is used to iteratively solve it. The incremental values of each variable obtained from the fourth order Runge-Kutta method are

$$T_{i+1} = T_i + \frac{\Delta x}{6} \left[\left(\frac{dT}{dx} \right)_1 + 2 \left(\frac{dT}{dx} \right)_2 + 2 \left(\frac{dT}{dx} \right)_3 + \left(\frac{dT}{dx} \right)_4 \right] \quad (28)$$

$$P_{i+1} = P_i + \frac{\Delta x}{6} \left[\left(\frac{dP}{dx} \right)_1 + 2 \left(\frac{dP}{dx} \right)_2 + 2 \left(\frac{dP}{dx} \right)_3 + \left(\frac{dP}{dx} \right)_4 \right] \quad (29)$$

$$w_{i+1} = w_i + \frac{\Delta x}{6} \left[\left(\frac{dw}{dx} \right)_1 + 2 \left(\frac{dw}{dx} \right)_2 + 2 \left(\frac{dw}{dx} \right)_3 + \left(\frac{dw}{dx} \right)_4 \right] \quad (30)$$

To obtain the hydraulic and thermal distribution along the pipeline, the fourth-order Runge-Kutta method is used repeatedly by setting the step size appropriately based on the pipe length.

3.2 Numerical solution of transient flow

In this study, the implicit central difference method is utilized to establish a difference equation system. Figure 3 illustrates the grid diagram of the differential method, where variables at time step j are known variables and variables at time step $j+1$ are variables to be solved. The

difference format for variables such as M can be obtained as follows:

$$\frac{\partial M}{\partial x} = \frac{M_{i+1,j} - M_{i,j} + M_{i+1,j+1} - M_{i,j+1}}{2\Delta x} \quad (31)$$

$$\frac{\partial M}{\partial \tau} = \frac{M_{i,j+1} - M_{i,j} + M_{i+1,j+1} - M_{i+1,j}}{2\Delta \tau} \quad (32)$$

$$M = \frac{M_{i+1,j} + M_{i,j} + M_{i+1,j+1} + M_{i,j+1}}{4} \quad (33)$$

for the $\frac{M|M|}{\rho}$ term in the momentum equation, we

have

$$\begin{aligned} \frac{M|M|}{\rho} = & \frac{1}{4} \left(\frac{M_{i,j}|M_{i,j}|}{\rho_{i,j}} + \frac{M_{i,j+1}|M_{i,j+1}|}{\rho_{i,j+1}} \right. \\ & \left. + \frac{M_{i+1,j}|M_{i+1,j}|}{\rho_{i+1,j}} + \frac{M_{i+1,j+1}|M_{i+1,j+1}|}{\rho_{i+1,j+1}} \right) \end{aligned} \quad (34)$$

Introducing grid ratio $\gamma = \frac{\Delta \tau}{\Delta x}$ to transform the Eqs. (16)

to (18) into difference forms, we obtain

$$\begin{aligned} F_1 = & (\rho_{i,j+1} - \rho_{i,j} + \rho_{i+1,j+1} - \rho_{i+1,j}) \\ & + \frac{\gamma}{A} (\rho_{i+1,j} - \rho_{i,j} + \rho_{i+1,j+1} - \rho_{i,j+1}) = 0 \end{aligned} \quad (35)$$

$$\begin{aligned} F_2 = & (M_{i,j+1} - M_{i,j} + M_{i+1,j+1} - M_{i+1,j}) \\ & + A\gamma(P(\rho_{i+1,j+1}, T_{i+1,j+1}) - P(\rho_{i,j+1}, T_{i,j+1})) \\ & + P(\rho_{i+1,j}, T_{i+1,j}) - P(\rho_{i,j}, T_{i,j}) \\ & + \frac{\gamma}{A} \left(\frac{M_{i+1,j+1}^2}{\rho_{i+1,j+1}} - \frac{M_{i,j+1}^2}{\rho_{i,j+1}} + \frac{M_{i+1,j}^2}{\rho_{i+1,j}} - \frac{M_{i,j}^2}{\rho_{i,j}} \right) \\ & + \frac{\lambda \Delta \tau}{4DA} \left(\frac{M_{i,j}|M_{i,j}|}{\rho_{i,j}} + \frac{M_{i,j+1}|M_{i,j+1}|}{\rho_{i,j+1}} \right. \\ & \left. + \frac{M_{i+1,j}|M_{i+1,j}|}{\rho_{i+1,j}} + \frac{M_{i+1,j+1}|M_{i+1,j+1}|}{\rho_{i+1,j+1}} \right) = 0 \end{aligned} \quad (36)$$

$$\begin{aligned} F_3 = & \rho_{i+1,j+1}h(\rho_{i+1,j+1}, T_{i+1,j+1}) - \rho_{i+1,j}h(\rho_{i+1,j}, T_{i+1,j}) \\ & + \rho_{i,j+1}h(\rho_{i,j+1}, T_{i,j+1}) - \rho_{i,j}h(\rho_{i,j}, T_{i,j}) \\ & - (P(\rho_{i+1,j+1}, T_{i+1,j+1}) - P(\rho_{i+1,j}, T_{i+1,j})) \\ & + P(\rho_{i,j+1}, T_{i,j+1}) - P(\rho_{i,j}, T_{i,j}) \\ & + \frac{1}{2A^2} \left(\frac{M_{i+1,j+1}^2}{\rho_{i+1,j+1}} - \frac{M_{i+1,j}^2}{\rho_{i+1,j}} + \frac{M_{i+1,j}^2}{\rho_{i+1,j}} - \frac{M_{i,j}^2}{\rho_{i,j}} \right) \\ & + \frac{\gamma}{A} (M_{i+1,j+1}h(\rho_{i+1,j+1}, T_{i+1,j+1}) \\ & - M_{i,j+1}h(\rho_{i,j+1}, T_{i,j+1}) + M_{i+1,j}h(\rho_{i+1,j}, T_{i+1,j}) \\ & - M_{i,j}h(\rho_{i,j}, T_{i,j})) \\ & + \frac{r}{2A^3} \left(\frac{M_{i+1,j+1}^3}{\rho_{i+1,j+1}^2} - \frac{M_{i,j+1}^3}{\rho_{i,j+1}^2} + \frac{M_{i+1,j}^3}{\rho_{i+1,j}^2} - \frac{M_{i,j}^3}{\rho_{i,j}^2} \right) \\ & + \frac{2K\Delta \tau}{D} (T_{i+1,j} + T_{i,j} + T_{i+1,j+1} + T_{i,j+1} - 4T_0) = 0 \end{aligned} \quad (37)$$

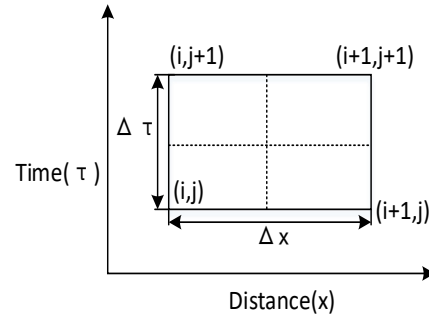


Fig. 3. Implicit central difference grid scheme

When boundary conditions are specified, a closed nonlinear system of equations can be formed by the difference equations and boundary conditions. This equation system is iteratively solved using the Newton-Raphson method. Let the iteration function column be

$$F = [F_1, F_2, \dots, F_n]^T, \quad \text{the iteration variable be}$$

$$X = [x_1, x_2, \dots, x_n]^T, \quad \text{the iteration increment be}$$

$$\Delta X = [\Delta x_1, \Delta x_2, \dots, \Delta x_n]^T, \quad \text{and } n \text{ be the sum of unknown}$$

variables. The iterative formula of Newton-Raphson are

$$X^k = X^{k-1} - \frac{F}{F'} \quad (38)$$

$$X^k - X^{k-1} = -\Delta X^{k-1} = -\frac{F}{F'} \quad (39)$$

$$X^k = X^{k-1} - \Delta X^{k-1} \quad (40)$$

where the iterative increment ΔX satisfies the following equation:

$$J^k \Delta X^k = F^k \quad (41)$$

where k is the number of iterations; J is the Jacobian matrix of the iterative function column F with respect to the iterative variable X, which has the following form:

$$J(X) = \begin{bmatrix} \frac{\partial F_1}{\partial x_1} & \frac{\partial F_1}{\partial x_2} & \dots & \frac{\partial F_1}{\partial x_n} \\ \frac{\partial F_2}{\partial x_1} & \frac{\partial F_2}{\partial x_2} & \dots & \frac{\partial F_2}{\partial x_n} \\ \vdots & \vdots & \ddots & \vdots \\ \frac{\partial F_n}{\partial x_1} & \frac{\partial F_n}{\partial x_2} & \dots & \frac{\partial F_n}{\partial x_n} \end{bmatrix} \quad (42)$$

In this study, the vector increment ΔX is

$$\Delta X = [\Delta\rho_{1,1}, \Delta T_{1,1}, \Delta M_{1,1}, \Delta\rho_{1,2}, \Delta T_{1,2}, \Delta M_{1,2}, \Delta\rho_{2,1}, \Delta T_{2,1}, \Delta M_{2,1}, \Delta\rho_{2,2}, \Delta T_{2,2}, \Delta M_{2,2}, \dots, \Delta\rho_{n,1}, \Delta T_{n,1}, \Delta M_{n,1}, \Delta\rho_{n,2}, \Delta T_{n,2}, \Delta M_{n,2}]^T$$

the function vector F is

$$F = [F_1, F_2, \dots, F_n, BF_1, BF_2, \dots, BF_n]^T$$

Based on the above methods, C++ is used for modeling and calculation. Fig. 4 shows the program flow.

4. MODEL VALIDATION

In this section, we employ the model to compute hydraulic and thermal changes along the supercritical CO₂ long-distance pipeline under working conditions of pipeline flow fluctuations. We compare and analyze the

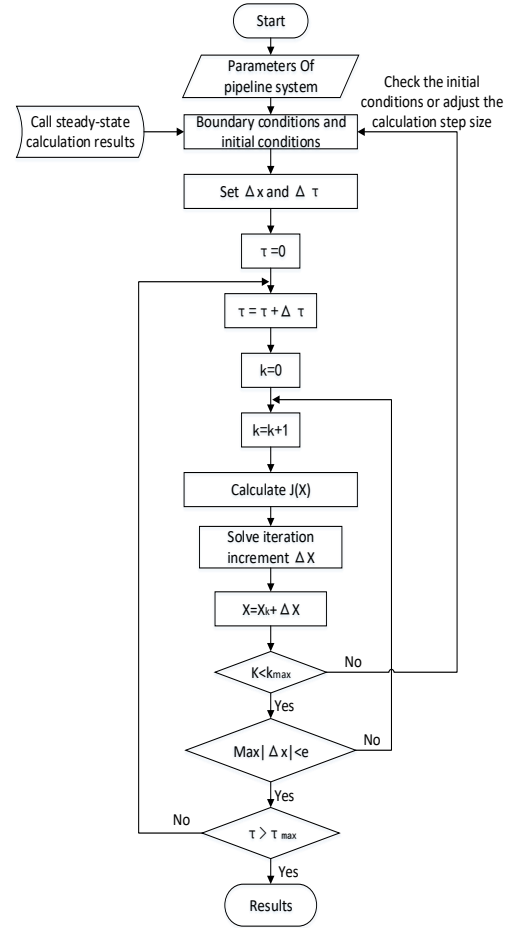


Fig. 4 program flow of calculation

4.1 Case introduce

The case simulated in this study refers to an actual operation of the supercritical CO₂ pipeline to set the simulated working conditions and pipeline parameter. The parameters of the pipeline are shown in Table 1.

Table 1

Parameters of the pipeline

| Pipe | Length(km) | inner diameter(mm) | Thickness(mm) | Ke(mm) | ρ (kg/m ³) | λ (W/(m K)) |
|------------------|------------|--------------------|---------------|--------|-----------------------------|---------------------|
| Steel API 5L X70 | 80 | 299 | 12 | 0.06 | 7830 | 45.3 |

simulation results with existing engineering flow simulation software, OLGA, to verify the accuracy of the model.

In this study, we assume that the pipeline is buried, with a height of 1.5m from the center of the pipeline to the ground, an average annual ground temperature of 15 °C, and the soil with a thermal conductivity of 1.6 (W/(m K)). The pipeline has no external coating and terrain fluctuations are not considered. The composition

of the pipeline medium in this study is shown in Table 2, which refers to the medium composition in the currently operating carbon dioxide pipeline transportation project.

4.2 Numerical simulation calculation and analysis

In this section, the proposed model and OLGA software are utilized to simulate the pipeline operating conditions

monitor the outlet temperature and pressure at the end of the pipeline.

Let us set the outlet mass flow to fluctuate according to the following formula:

$$M = M_0 \times 0.2 \sin\left(\frac{\tau}{1000} \pi\right) + M_0 \quad (43)$$

The simulation results for operating conditions A and B using both the developed model and OLGA software are shown in Figures 5 and 6. It is observed that the developed model produced higher outlet pressure values than OLGA in both simulations. Specifically, at the end of the simulations, the developed model showed pressure values 1.83 bar and 2.78 bar higher than OLGA for the two working conditions, respectively. On the other hand, the developed model calculated lower outlet temperature values than OLGA, with differences of 2.67K and 1.76K for the two working conditions, respectively.

Table 2
Medium composition in the pipeline

| Components | Molar percentage |
|------------------|------------------|
| CO ₂ | 99.2 |
| CO | 0.043 |
| H ₂ | 0.006 |
| H ₂ S | 0.0009 |
| H ₂ O | 0.0001 |
| CH ₄ | 0.2 |
| Ar | 0.01 |
| N ₂ | 0.54 |

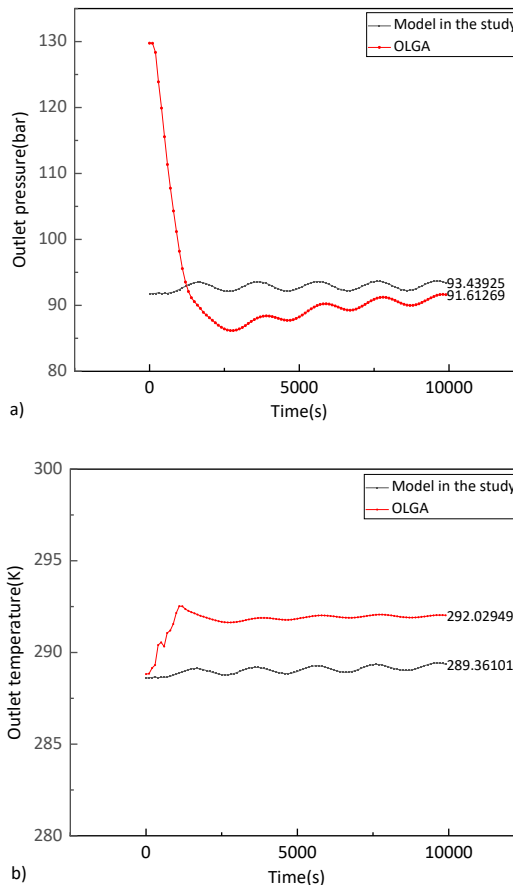


Fig. 5. Variation of outlet pressure and temperature in operating conditions A:(a) Variation of outlet pressure, (b) Variation of outlet temperature.

outlined in Table 3 and Eq. (43), and to dynamically

Table 3

Parameters of the pipeline

| Operating conditions | $T_{inlet}(K)$ | $P_{inlet}(MPa)$ | $M_0(kg/s)$ | $Q(t/a)$ | simulation time(s) |
|----------------------|----------------|------------------|-------------|----------|--------------------|
| A | 323.15 | 9.5 | 24.3 | 700000 | 10000 |
| B | 313.15 | 11 | 34.2 | 1000000 | 10000 |

Additionally, Figure 5 illustrates that OLGA requires a longer pre-simulation period to reach a stable state compared to the developed model, which reaches a stable state faster.

5. DISCUSSION

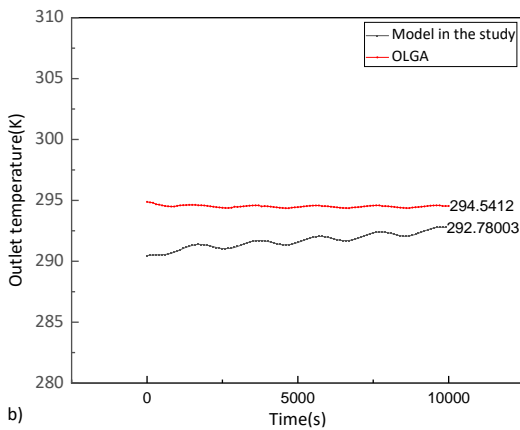
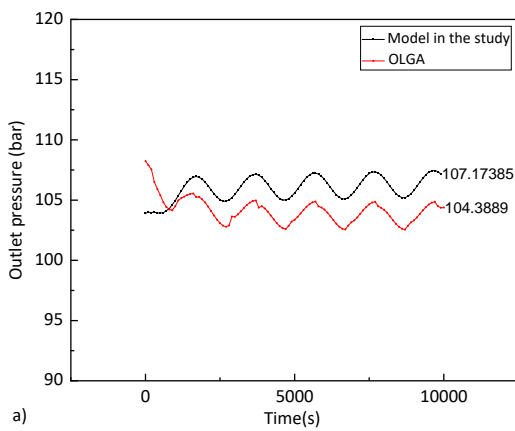


Fig. 6. Variation of outlet pressure and temperature in operating conditions B:(a) Variation of outlet pressure, (b) Variation of outlet temperature.

Through comparison of the simulation results obtained using OLGA software with those obtained using the proposed model, a minor discrepancy was observed between the two. However, the lack of real on-site data impedes the accurate determination of the accuracy of

the two. Notably, the proposed model achieves a stable simulation state faster and requires considerably less pre-simulation time than OLGA. This is due to the application of steady-state simulation before transient simulation, resulting in initial conditions of the transient simulation that are closer to the stable simulation state. In terms of computational speed, however, under the same hardware conditions, OLGA software performs calculations more rapidly than the proposed model, as the numerical solution method of the model necessitates the solution of a large sparse system of equations in every iteration.

6. CONCLUSION

This study, using numerical solution technology and C++ programming, established a hydraulic and thermodynamic calculation model for slow transient transportation of supercritical CO₂ pipelines, which has good calculation accuracy. This study presents a valuable contribution to the field of slow transient transportation of supercritical CO₂ pipelines. The proposed model has the potential to be applied in practical engineering projects and offers valuable guidance for further research and development of numerical simulation technology in this field.

ACKNOWLEDGEMENT

I would like to thank my mentor Professor Hu Qihui for his careful guidance and patient revision of the ideas and content of this paper. At the same time, I would like to express my special gratitude to Professor Zhu Jianlu in our research group for his theoretical guidance on this article.

DECLARATION OF INTEREST STATEMENT

The authors declare that they have no known competing financial interests or personal relationships that could have appeared to influence the work reported in this paper. All authors read and approved the final

manuscript.

REFERENCE

- [1] Liu M, Teng L, Li Y, et al. Study on hydraulic models and characteristics suitable for supercritical CO₂ pipeline transportation. *Oil and Gas Field Surface Engineering*. 2016;35(6):14-17.
- [2] Wang Quande. Research on simulation application of long distance supercritical CO₂ pipeline transportation [D]. Xi'an University of Petroleum, 2020.
- [3] Chen B, Fang Q, Bai S. Factors affecting the shutdown of supercritical CO₂ transportation pipelines containing impurities. *Nat Gas Chem Ind*. 2020;45(3):84-89.
- [4] Chen B, Xu Y, Bai S. Research on Transient Characteristics of supercritical CO₂ leakage process in pipeline transportation. *Petrol Mach*. 2020;48(8):136-142.
- [5] Chen B, Fang Q, Xu Y. Simulation of hydrate particle movement in supercritical CO₂ transportation pipeline. *J Xi'an Petrol Univ (Nat Sci Ed)*. 2021;36(5):114-120.
- [6] Chen, B., Xu, M., Fang, Q., & Bai, S.. The effect of shutdown and restart of supercritical CO₂ pipeline network containing impurities on hydrate generation. *Petroleum and Natural Gas Chemicals*, 2022; 51(4):43-50.
- [7] Gu S, Li Y, Teng L, et al. A new model for predicting the decompression behavior of CO₂ mixtures in various phases. *Process Saf. Environ. Prot* 2018; 120:237-247.
- [8] Chaczykowski, M., & Osiadacz, A. J, Dynamic simulation of pipelines containing dense phase/supercritical CO₂ rich mixtures for carbon capture and storage, *Int. J. Greenhouse Gas Control* 2012; 9,:446-456.
- [9] Li, C., Zhang, Y., Jia, W., et al. Online simulation method and software development for large-scale natural gas pipeline network systems. *Oil and Gas Storage and Transportation*, 2022; 41 (6): 723-731.
- [10] Colebrook, C.F. Turbulent flow in pipes, with particular reference to the transition region between the smooth and rough pipe laws. *J Inst. Civil Eng* 1939; 11:133-156.
- [11] Li, Y., & Yao, G. Gas pipeline design and management. 2nd ed. China University of Petroleum Press, 2015.
- [12] YAWS, C.L. Chemical properties handbook, Beijing World Book Publishing Company Beijing Company, 1999.
- [13] Smith, J.M , Van Ness, H.C , Abbott M.M . Introduction to Chemical Engineering Thermodynamics. 6th ed. New York: McGraw Hill, 2001.
- [14] Yu, Z., Li, X., Lan, Z., et al. Calculate the residual enthalpy and residual entropy of gases using the equation of state method. *Chemical Times*, 2016; 30 (4): 12-14.
- [15] Chen S. A program development for unsteady gas flowanalysis in complex pipe networks. R&D Center, Korea Gas Corporation, 2000.